Optical Fiber Technology 77 (2023) 103161

Contents lists available at ScienceDirect

Optical Fiber Technology

journal homepage: www.elsevier.com/locate/yofte

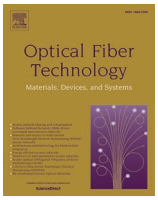

Demonstration of M-QAM OFDM bidirectional 60/25 GHz transmission over 10 km Fiber, 100 m FSO and 2 m radio seamless heterogeneous fronthaul link

L. Vallejo [a,b,*], B. Ortega [a], J. Mora [a], D.-N. Nguyen [c,d], C. Guerra [c], J. Bohata [c], J. Spacil [c], S. Zvanovec [c]

[a] Instituto de Telecomunicaciones y Aplicaciones Multimedia, Universitat Politecnica de Valencia, Cno. de Vera, s/n, 46022, Valencia, Spain
[b] DSP Centre of Excellence, School of Computer Science and Electronic Engineering, Bangor University, Dean Street, Bangor, Gwynedd, LL57 1UT, United Kingdom
[c] Department of Electromagnetic Field, Faculty of Electrical Engineering, Czech Technical University in Prague, Technicka 2, 166 27, Prague, Czech Republic
[d] II-VI Incorporated (now is Coherent Corp.), 36 VSIP Street 4, Vietnam-Singapore Industrial Park, Thuan An City, Binh Duong Province, Vietnam

ARTICLE INFO

Keywords:
Free space optics
Optical fiber
5G
Millimeter wave
Full-duplex
Fronthaul

ABSTRACT

In this paper, we demonstrate the experimental transmission of 16- and 64- quadrature amplitude modulation (QAM) Long Term Evolution - Orthogonal Frequency Division Multiplexing (LTE-OFDM) signals by using millimetre wave frequencies at 60 GHz and 25 GHz for downlink and uplink, respectively, over a heterogeneous optical fronthaul infrastructure. A directly modulated laser was employed for both links, which enables the cost-effective full-duplex system proposal. The bidirectional link consists of a 10 km of single mode fiber, a 100 m long free space optics channel and 2 m long wireless radio link, which brings flexibility for future wireless networks. The error vector magnitude (EVM) parameter is measured for a range of the received optical and electrical power as well as the signal-to-noise ratio. A comprehensive estimation of penalty factors in the different network segments is presented. The successful transmission over the whole proposed network with the EVM below the required limit of 9 % for 64-QAM with 20 MHz bandwidth is experimentally demonstrated for the received optical power of −2.7 dBm and −1 dBm for the downlink and uplink, respectively.

1. Introduction

The fifth generation (5G) of mobile networks is under current deployment in major urban centers all over the globe and relies on a very dense network utilising new technologies such as millimeter wave (mmW), network function virtualization, software-defined networks, network slicing and massive multiple-input multiple-output (mMIMO).

The 5G features can be broadly categorized into three main service classes: enhanced mobile broadband up to 20 Gbps; ultra-reliable low-latency communications with 99.999 % reliability and < 1 ms latency; and massive machine-type communications up to 106 devices/km^2 [1].

However, it is expected that the total mobile users will reach 17.1 billion with around 250 GB of average data consumption per user per month by 2030 [2], where a new paradigm with Internet of Things, smart manufacturing, industrial automation, tactile internet, holographic communications, e-Health and augmented, and virtual reality, amongst other services, will impose huge requirements which will not be satisfied by the currently implemented 5G technology.

In order to meet the increasing data rates and number of users, the next networks' standards are expected to include especially additional spectrum (i.e., mmW, THz, visible, and wireless infrared) with dynamic management, new air interfaces with many smaller cells (i.e., coordinated multi-point, intelligent reflective surfaces and cell-free mMIMO), 3D coverage, energy efficient communications, mobile convergence, and integrated technology solutions. Accordingly, the network infrastructure is expected to be flexible, smart, and open to multi-vendor equipment by the softwarization and virtualization, in the so-called open radio access network architecture and a new paradigm opens up with the integration of artificial intelligence, blockchain, digital twin, and mobile networks [1].

The effective architecture for 5G networks is the centralized radio access network (C-RAN), where the backhaul link connects the central office (CO) to the core network, as depicted in Fig. 1, and the fronthaul link connects the CO to the radio units (RUs) [3]. It is possible to employ

* Corresponding author.
E-mail address: luivalc2@iteam.upv.es (L. Vallejo).

https://doi.org/10.1016/j.yofte.2022.103161
Received 7 July 2022; Received in revised form 19 September 2022; Accepted 16 November 2022

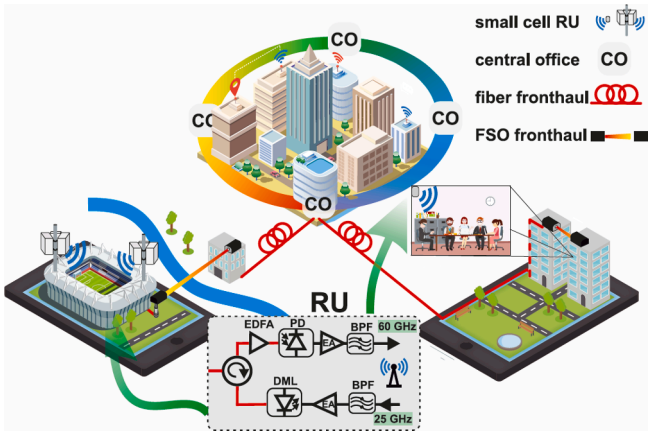

Fig. 1. Schematic of a C-RAN with fronthaul links based on fiber and FSO. RU: Radio unit, CO: central office, FSO: free space optics, DML: directly modulated laser, EA: electrical amplifier, BPF: bandpass filter, PD: photodiode, EDFA: erbium doped fiber amplifier.

radio over fiber (RoF) technology to transport and distribute digital and/or analog signals among the CO and the RUs via optical fiber links. It can be further extended to employ free space optics (FSO) links in the so-called radio-over-FSO (RoFSO) to provide fixed/wireless convergence with sufficient bandwidth to deliver high speed services over long distances at a low cost, with high reliability and low latency [4]. Within this concept, the signal is photodetected at a base station before being radiated, giving rise to a fiber-FSO-wireless heterogeneous network. An analog RoF provides a simple and scalable solution for the fronthaul link with no need for an analog-to-digital converter and digital-to-analog converter, neither at the RUs nor the CO [5].

The use of mmW frequency signals has been introduced by the 5G new radio access technology due to the large spectral availability and achievable throughput and is also considered as an enabling technology for the future deployment of 6G networks [6]. The shorter wavelength leads to a smaller antenna size, which allows an increase in the dimension of the arrays (number of antenna elements), and therefore, to narrow the beams. Current standardization efforts are mainly focused on the 60 GHz band, e.g., the ECMA-387, the IEEE 802.15.3c and the IEEE 802.11ad [7], although other bands with low attenuation (i.e., 35 or 94 GHz) are also very attractive for concrete use cases. Aperture antennas, i.e., reflector, lens and horn, are widely employed in applications such as point-to-point and relay-aided communications because of their high gain, wide bandwidth and simple structure, but nonlinear distortions and phase noise are major challenges in the design of integrated circuits. Additionally, the Line-of-Sight (LoS) requirement and poor diffraction properties at these wavelengths lead to strong blockage in typical access network scenarios that can be overcome by using highly directive antenna arrays [8].

Moreover, photonic approaches for mmW signal generation have been successfully demonstrated in the literature to overcome some of the major challenges related to electronics limitations at those high frequencies, from the basic heterodyne beating approach up to more sophisticated systems employing nonlinear effects [9]. In particular, the optical frequency multiplication based on an electro-optical Mach Zehnder modulator (MZM) represents an excellent solution in terms of cost and complexity [10].

During the last decade, large efforts have been done in the literature toward the experimental demonstration of signal transmission over mmW signals. Table 1 summarises the employed carrier frequencies, waveforms and achieved bitrates, fronthauls types, antenna wireless distance and if they considered as well the uplink (UL) transmission. Purely electric signal generation with simple and compact transceivers exhibits limited transmission rates, while microwave photonics-based signal generation (MWPG) techniques provide a higher transmission rate, wider operation frequency, tunability, and stability [11–15].

To the best of the authors knowledge, this paper presents the first experimental demonstration of data transmission over mmW frequencies for the downlink (DL) and the UL between the CO and the user where optical transmission is held along a 10 km standard single mode fiber (SMF), 100 m FSO and 2 m seamless wireless link; and 16- and 64-

Table 1
Experimental demonstrations of data transmission over mmw signals. NRZ: non-return-to-zero, SSMF: standard single mode fiber, PDM: polarization division multiplexing, QAM: quadrature amplitude modulation, QPSK: quadrature phase shift keying, LTE: long term evolution, ASK: amplitude shift keying, OOK: on–off keying.

	MWPG	Waveform	Frequency	Optical fronthaul	RF Wireless	Uplink
[11]	Yes	155 Mb/s NRZ	62.5 GHz	25 km SSMF	1.5 m	Yes
[12]	Yes	PDM 16-QAM 100 Gb/s	87.5 GHz	No	1.20 m	No
[13]	Yes	112 Gb/s PDM-16QAM 108 Gb/s PDM-QPSK	37.5 / 100 GHz	80 km SSMF	1.5 / 0.7 m	No
[14]	Yes	PDM 16-QAM 128 Gb/s	100 GHz	50 km SSMF	1 m	No
[15]	Yes	LTE-A 20 MHz	92.5 / 96 GHz	10 km SSMF	3 m	Yes
[16]	No	16-QAM 56 Gb/s	68 / 102 GHz	No	No	No
[17]	Yes	PDM 64-QAM 100 Gb/s	57.2 GHz	60 km SSMF	1 m	No
[18]	No	64-QAM 10 Gb/s	71–86 GHz	No	Estimated 1 km	No
[19]	No	ASK 15 Gb/s	84 GHz	No	50 cm	No
[20]	No	16-/64-QAM 28 Gb/s	60 GHz	No	10 cm	No
[21]	Yes	1 Tb/s	124.5 /150.5 GHz	10 km SSMF	3.1 m	No
[22]	No	OOK 12.5 Gb/s	60 GHz	No	2 cm	No
[23]	Yes	4096-QAM 45 Gb/s	83.5 / 73.3 GHz	No	13.4 m	Yes
[24]	Yes	16.5 Gb/s 32-QAM	60 GHz	50 Km SSMF	3 m	No
[25]	Yes	10 Gb/s	60 GHz / 1.1 THz	50 Km SSMF/100 m FSO	No	Yes
[26]	Yes	12.5 Gb/s / 6.5 Gb/s	60 GHz / 30 GHz	80 Km SSMF	110 m / 50 m	Yes
[27]	Yes	M−QAM 36 Gb/s	47.27 GHz	50 km SSMF	9 m	No
[28]	Yes	10 GHz 16-QAM OFDM	50 GHz	20 km SSMF	2 m	No
This paper	Yes	64-QAM LTE 20 MHz	60 / 25 GHz	10 km SSMF / 100 m FSO	2 m	Yes

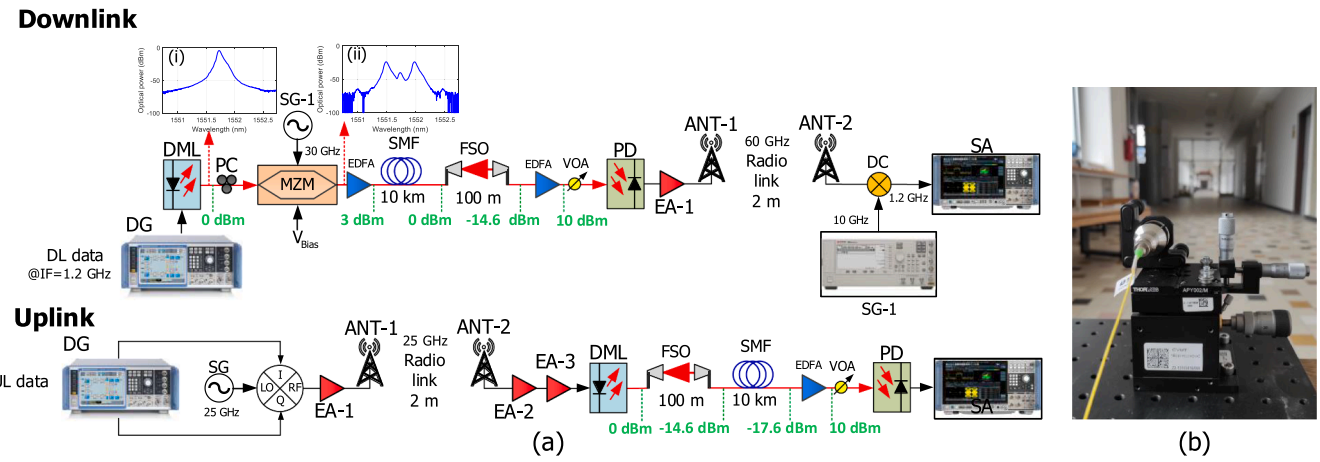

Fig. 2. (a) Experimental setup: Downlink at 60 GHz and uplink at 25 GHz bands and (b) Photograph of the coupling from fiber to FSO. Insets show the signal spectra: (i) DML output, (ii) MZM output. DG: digital generator, DML: directly modulated laser, PC: polarization controller, MZM: Mach-Zehnder modulator, SG: signal generator, SMF: single mode fiber, FSO: free space optics, EDFA: erbium doped amplifier, VOA: variable optical attenuator, PD: photodetector, EA: electrical amplifier, SA: signal analyser.

quadrature amplitude modulation (QAM) Long Term Evolution - Orthogonal Frequency Division Multiplexing (LTE-OFDM) signals are transmitted as a proof of concept. Moreover, the directly modulated laser (DML) used for the UL mmW transmission is presented to provide an effective approach in terms of the performance, cost and complexity.

The paper is structured as follows: Section II describes the experimental setup and the parameters employed for the DL and UL signal transmission while Section III presents the experimental results demonstrating the error vector magnitude (EVM) performance of the bidirectional link and the evaluation of optical and electrical power requirements for 16 and 64-QAM modulation formats. Finally, Section IV summarizes the main achievements of the paper as the main conclusions of the paper.

2. Description of the millimeter wave hybrid bidirectional link

A heterogeneous system for mmW signal transmission based on a 10 km SMF, 100 m FSO and 2 m radio seamless wireless links was set up to demonstrate bidirectional signal performance. The proposed setup is shown in Fig. 2. As depicted in Fig. 2(a), the DL employs a DML, which is a monolithically-integrated passive feedback laser described in [29], centered at 1551.7 nm (the optical spectrum is shown in inset (i) of Fig. 2) and driven through a bias tee (SigTek SB12D2) by an electrical M-QAM OFDM long term evolution (LTE) data signal carried by an intermediate frequency (IF) of 1.2 GHz which is generated by a vector data signal generator (DG, R&S SMW200A). The MWPG approach based on carrier-suppressed external modulation is employed for the frequency up-conversion of the DML output signal where the frequency of the electrical driving signal at the Mach-Zehnder modulator (MZM, Optilab IML-1550–50-PM) is $f_{RF} = f_{mmW}/2 = 30$ GHz, where f_{mmW} is the target frequency band. The MZM output signal, whose spectrum is shown in inset (ii) of Fig. 2, is transmitted over the 10 km long SMF section and the FSO link, which was realized by two doublet collimators (Thorlabs F810APC-1550) with the total FSO insertion loss of 14.6 dB. Note that the FSO link was tested indoor so that any environmental effect could be neglected. After the FSO link, the signal is launched into an erbium doped fiber amplifier (EDFA) to compensate for the optical losses as a post-amplification stage, and then a variable optical attenuator (VOA) allows to adjust the received optical power (RoP) after the EDFA. Note the EDFA can also be placed at the transmitting side, which is a cost-

Table 2
Experimental parameters.

DOWNLINK			UPLINK		
DG	20 MHz 16, 64-QAM LTE		DG	20 MHz, 64-QAM LTE	
	IF	1.2 GHz			
	P_{data}	5 dBm (OB2B) −12 dBm (others)		V_{data} (IQ)	0.5 V
SG	f_{RF}	30 GHz	SG	f_{RF}	25 GHz
	P_{LO}	24 dBm		P_{LO}	18 dBm
DML	λ	1551.7 nm	Radio link	L_{RF}	2 m
	BW	33 GHz			
	P_{DML}	0 dBm	EA1	G_{EA1}	28.5 dB @25 GHz
SMF	L_{SMF}	10 km	EA2	G_{EA2}	29 dB @ 25 GHz
			EA3	G_{EA3}	29 dB @ 25 GHz
	α	0.2 dB/km	DML	BW	33 GHz
FSO	L_{FSO}	100 m		P_{DML}	0 dBm
	α_{FSO}	14.6 dB		λ	1551.7 nm
EDFA	P_{out}	10 dBm	FSO	L_{FSO}	100 m
				α_{FSO}	14.6 dB
PD	BW	70 GHz	EDFA	P_{out}	10 dBm
	R	0.6 A/W	SMF	L_{SMF}	10 km
EA1	G_{EA1}	35 dB @ 60 GHz		α	0.2 dB/km
	NF_{EA1}	5 dB	PD	BW	33 GHz
RF link	L_{RF}	2 m		R	0.72
ANT	BW	60–90 GHz	ANT	BW	4–40 GHz
	Gain	25 dBi @60 GHz		Gain @25 GHz	14.2 dBi

effective deployment due to the possibility to share resources. The photodiode (PD, Finisar XPDV3120) performs the opto-electrical conversion where both $\pm f_{RF}$ sidebands of the modulated optical signal beat each other to generate the desired $f_{mmW} = 2f_{RF} \mp f_{IF}$, where lower and upper data bands are located at 58.8 GHz and 61.2 GHz, respectively.

Then, the signal is amplified by a low-noise electrical amplifier (EA, SAGE SBL-5037033550-VFVF-S1) and radiated by a pyramidal horn antenna (RF spin, H-A90-W25) over a 2 m long wireless radio link. Finally, the same type of the receiving antenna allows the signal reception and the further analysis is accomplished in the signal analyser (SA, R&S FSW). An electrical down-converter (DC, R&S FS-Z90) is used before the signal analysis due to the frequency limitation of the available instrumentation. The experimental parameters are fully detailed in Table 2 for every component employed in the setup.

Fig. 2(a) shows the setup for the UL operating at 25 GHz, which employs the same DG as in the DL to generate a fixed I/Q signal output which is combined with the local oscillator signal at 25 GHz by using an RF mixer. Note that the DL and UL were not measured simultaneously. The resulting signal is amplified by EA-1 (Wisewave AGP-33142325–01) and transmitted by a double ridged horn antenna (RF spin DRH40) through the 2 m long wireless radio link. The received signal is amplified in two identical cascaded amplifiers (MITEQ AMF-4F-260400–40-10P) and launched into the DML, which is already described above, for electro-to-optical conversion prior to transmission over the wired and wireless optical links. The high bandwidth of the DML is here fully used to represent an effective solution for a low complexity UL system compared to the conventional usage of external modulation. In general, compared to the use of MZM, direct modulation offers satisfactory RF to optical conversion efficiency and linearity but has relatively low output power and the modulation chirp is generally higher. Finally, an EDFA and a VOA are also used to compensate the losses and adjust the optical power at the PD, which performs the opto-to-electronic conversion. The recovered data are then analysed in the SA. Table 2 summarises the main experimental parameters employed in the setup.

An experimental study on the optimisation for each link was crucial to assure the correct performance. More concretely, a radio signal, composed of LTE test model 3.1 with the bandwidth of 20 MHz and variable electrical power, P_{data}, at 1.2 GHz IF was employed for the DL characterization. Note that the predefined test model TM 3.1, designated for testing the base stations, employs OFDM signals with 64-QAM modulation [30]. The obtained results from the characterization are shown in Fig. 3. Optical back-to-back (OB2B), consisting of the setup shown in Fig. 2(a) for the DL without SMF, FSO and radio link, evinces a minimum EVM value for a given $P_{data} = 5$ dBm under constant RoP = -3 dBm. As expected, the EVM at first decreases with increasing electrical power due to corresponding higher to signal-to-noise ratio (SNR), but for P_{data} above 5 dBm, the EVM starts to increase due to the nonlinear distortion introduced by the DG and the DML at higher power levels. The same behaviour is also observed when the fiber is included in the OB2B setup, denoted as SMF in Fig. 3. However, there can be seen a shift of the curves due to the dispersion effects over the DML distorted output signal. This characterisation was repeated for the scenario based on SMF followed by the radio sub-link and for the full-link, which corresponds to the complete scheme in Fig. 2(a), i.e., including SMF, FSO and the radio sub-link. Nevertheless, for both scenarios which include the antenna link, i.e., the SMF + radio and full-link, the RoP was increased to 8 dBm to obtain acceptable EVM levels. Similar performance is expected in both curves provided the amount of losses is compensated by the addition of EDFAs and EAs in each scenario. Slight EVM differences are observed due to experimental drift of MZM response which leads to an RoP uncertainty close to ± 0.5 dB. The minimal EVM values are higher than in OB2B scenario due to the balance between the distortion effects and the current noise, namely shot noise. Therefore, the use of optimal P_{data} for a particular scenario is required, i.e., $P_{data} = -12$ dBm is employed for SMF, SMF + radio link, and full-link operation while 5 dBm is used for the OB2B scenario, as described in Table 2. The EVM limit for 64-QAM is indicated by a dashed horizontal line in Fig. 3.

Similar optimisation was also done for the UL direction. As described above, in this case the local oscillator (LO) at 25 GHz frequency was mixed with I and Q (IQ) data from the DG to create the mmW signal at the desired frequency while the radio signal for the UL was the same as for the DL optimization. More specifically, the electrical power of the LO, P_{LO}, was varied to obtain the EVM performance characterisation of the UL under different configurations and constant RoP of 8 dBm. Note that during the characterization, the IQ signal voltage was kept the same for all configurations, i.e., 0.5 V. The obtained curves in Fig. 4 show a similar EVM behaviour for all the scenarios, which are electrical B2B (EB2B), radio + OB2B, radio + SMF, and full-link. The different EVM levels at the $P_{LO} = 18$ dBm indicate the penalty introduced by the OB2B, SMF and SMF + FSO links with regards to the EB2B configuration, which is 2.9 %, 5.1 % and 6.4 % for the radio link + OB2B, radio link + SMF and full-link, respectively. An EVM peak at $P_{LO} = 15$ dBm is found due to the electrical RF mixer response, which is used for the UL mmW signal generation, given that it is shown also in the EB2B measurement where no optical components are involved. Regarding P_{LO}, the lowest EVM value is 7.3 % and was obtained under the full-link configuration with $P_{LO} = 18$ dBm and thus in this work we adopted this P_{LO} value, as detailed in Table 2, for further UL experiments. It is worth to mention that similar low EVM was recorded also for $P_{LO} = 7$ dBm, however we adopted $P_{LO} = 18$ dBm anyway in order to get higher electrical power in the receiver after optical transmission Note that the electrical input power in the cascade of the two amplifiers EA-2 and EA-3 (see Fig. 2(a)) after the receiving antenna in the UL is −56 dBm and −37 dBm for the $P_{LO} = 0$ dBm and $P_{LO} = 18$ dBm, respectively.

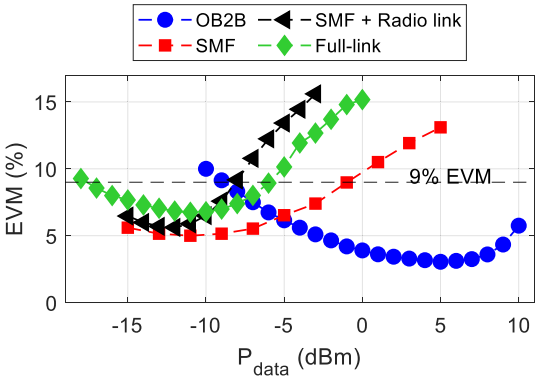

Fig. 3. DL Signal parameters optimization. Measurement of EVM vs P_{data} for OB2B and SMF: RoP = -3 dBm; SMF + radio and full-link: RoP = 8 dBm.

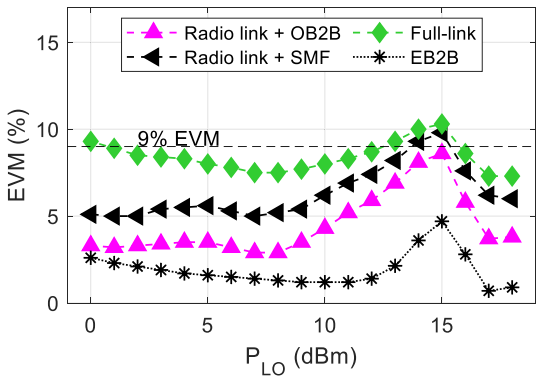

Fig. 4. UL signal parameters optimization: measurement of EVM vs P_{LO} for different configurations (RoP = 8 dBm) including the EB2B measurement.

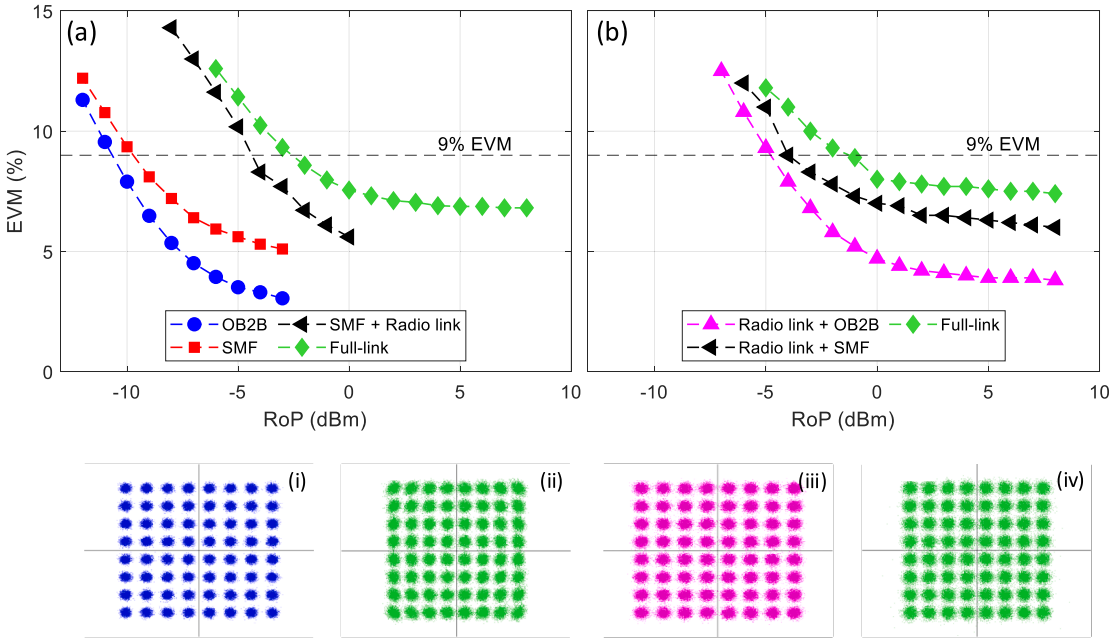

Fig. 5. EVM vs RoP for 64-QAM with different configuration in both links: (a) 61.2 GHz DL (b) 25 GHz UL. Corresponding insets show constellations for DL: (i) OB2B (RoP = -3 dBm), (ii) full-link (RoP = 8 dBm); and for UL: (iii) radio and OB2B (RoP = 3 dBm), (iv) full-link (RoP = 9 dBm).

3. Experimental transmission results

In the following part, both the DL and UL performances were characterised by measuring the dependence of the EVM on the RoP for a 64-QAM signal transmission in the 60 GHz band (DL) and in the 25 GHz band (UL). Note that according to the previous section, the DL OB2B scenario employed different P_{data} compared to other DL scenarios, i.e., 5 dBm vs −12 dBm, so the comparison between them is not straightforward. The results, illustrating the EVM dependence on the RoP obtained by introducing the optical loss of the VOA, for the DL and UL with a 64-QAM are depicted in Fig. 5. As expected, Fig. 5(a) shows that the DL EVM decreases with the increasing optical power while the SMF + radio and full-links imply a power penalty at the 9 % threshold of 5 and 7 dB, respectively, with regards to the SMF scenario power level. This is because the SMF + radio and full-link both contain the 2 m long radio link at 61 GHz, which deteriorates the overall EVM performance. The results imply that for the full-link scenario, the acceptable transmission quality requires a minimum RoP of −2.7 dBm. Note that the additional optical loss, introduced by the VOA, is 11 dB in this case. Fig. 5(b) then shows the EVM dependence on the RoP for UL where a penalty of 1.5 and 3 dB is observed when the SMF and full–links are introduced, respectively, with regard to the OB2B scenario. The required RoP, in this case, is −1 dBm for the full–link operation to keep the EVM below 9 %. Note that the maximal additional optical insertion loss is 10 dB in this case and thus 1 dB lower compared to the DL. The difference among particular UL scenarios is less significant, compared to the DL, because the radio link is involved in all of them due to the UL definition. Insets (i) and (ii) then show the 64-QAM constellations for the DL under the OB2B and full-link scenarios, respectively, while (iii) and (iv) depict the constellations for radio link + OB2B and full-link scenarios in UL, respectively. It should be emphasized that the transmission over the full-link in both the DL and UL setup fulfils the given EVM limit for a wide range of the RoP.

In the next step, the EVM characterisation is depicted also in terms of

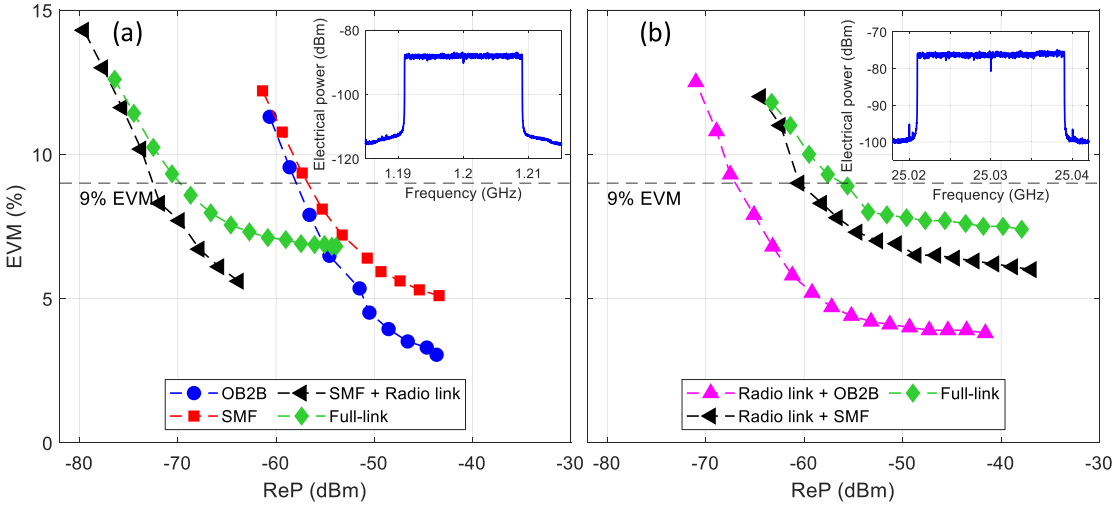

Fig. 6. EVM vs ReP for 64-QAM signal for: (a) 61 GHz DL, (b) 25 GHz UL. Insets depict corresponding electrical spectra obtained under full-link transmission (RoP = 8 dBm) with RBW = 10 kHz, where DL signal has been frequency downconverted to IF.

the received electrical power (ReP) in the mmW band for both DL and UL as shown in Fig. 6, while the different ReP values were set by adjusting the VOA like in the previous case. A slight degradation can be seen in Fig. 6(a) when only the SMF, i.e., without radio link, is included with respect to OB2B due to the propagation effects of the distorted signal at the DML output. Note that the EVM results experience a significant improvement in terms of ReP in those scenarios where the radio link is present due to the electrical amplification. In the case of the UL, the radio link is present in all scenarios, and therefore, Fig. 6(b) shows, -as in the case of the EVM vs RoP, similar performance results for all the scenarios compared to the DL. According to Fig. 6, the required ReP = −70 dBm and −57 dBm for the full DL and UL scenarios, respectively. In the DL, the minimal ReP to keep the EVM below 9 % is higher for the scenarios with radio links, i.e., SMF + radio link and full-link, which is caused by the different power budget in scenarios with and without seamless antenna link. On the other hand, the UL results for the RoP and ReP demonstrate similar behaviour with different EVM for a particular configuration and fixed ReP. In other words, radio link + OB2B requires lower RoP and ReP value than the radio link + SMF and full-link scenarios in order to keep the EVM under 9 %. It is because the radio link is employed in all the UL scenarios, as already described above. Corresponding insets in Fig. 6(a) and b) show the electrical spectra of full-link with RoP = 8 dBm, where the DL signal has been downconverted to IF before evaluating.

The DL characterization was done with the 64-QAM and 16-QAM modulation formats (LTE test model TM 3.2) and the EVM dependence on the SNR of the electrical recovered signal was measured to provide information about the distortions in the DL transmission system, compared with the only the 64–QAM format used for previous tests. Note that SNR was measured after photodetection by means of the SA. The 16–QAM performance in Fig. 7(a) shows very similar behaviour for all scenarios, with an estimation of the minimal required SNR above 22 dB to achieve EVM levels below the 13.5 % limit at 16-QAM. Further, Fig. 7(b) shows the corresponding results for the 64-QAM signal transmission, where a maximum 2.5 dB penalty is observed in the full-link characterization with respect to the OB2B link at the 9 % EVM limit. A minimal SNR of 23.7 dB is required for the correct transmission of the 64-QAM signal at 61 GHz for all the scenarios in the DL. Insets in Fig. 7(a) and (b) show the corresponding constellation diagrams of transmitted signals over the full-link with an SNR of 28 dB. As explained above, good EVM performance in the UL requires the maximization of the electrical power in the receiver and that leads to increased to higher amplifiers noise level and intermodulation distortion, which both affect the measured SNR magnitude. In this case, varying the optical losses does not provide valuable information with regards to the SNR, and therefore, EVM vs SNR is not shown for UL.

Table 3
Best achievements for 64-QAM signal transmission over DL and UL with full-link configuration (RoP = 8 dBm).

	ReP (dBm)	SNR (dB)	EVM (%)
DL	−54	28	6.8
UL	−38	n.a.	7.5

Finally, Table 3 summarises the best achievements obtained in the 64-QAM signal transmission experiments over full DL and UL in terms of RoP, ReP, SNR and EVM. We would like to emphasize the benefits of the employed DML in both DL and UL setups. For the DL, the DML is a very cost-effective solution, which reduces cost and complexity especially because it combines the laser and modulator into one device and even for the 61 GHz transmission, the DML with low-bandwidth, i.e., 1 GHz, is enough. Further, it benefits from the frequency doubling in the photonic generation approach, which requires only half input frequency, i.e., 30 GHz in the MZM to provide 61 GHz seamless transmission, resulting in a significant reduction of the equipment requirements. Additionally, the use of the high frequency bandwidth DML for the UL also reduces complexity and potential costs because the DML, having smaller footprint compared to the laser and MZM, can be produced in a large series and then become more affordable. Therefore, the radio unit in the cell site can be significantly simpler, as indicated in Fig. 1.

4. Conclusions

An experimental demonstration of an LTE M-QAM signal transmission over the 60 and 25 GHz bands for the DL and UL, respectively, is presented over an optical heterogeneous fronthaul network consisting of 10 km of optical fiber, a 100 m FSO link and a 2 m seamless radio link. The optimisation of the electrical signals in both DL and UL, and the comprehensive analysis of the results has been provided. The EVM measurements for both link directions under different configurations in

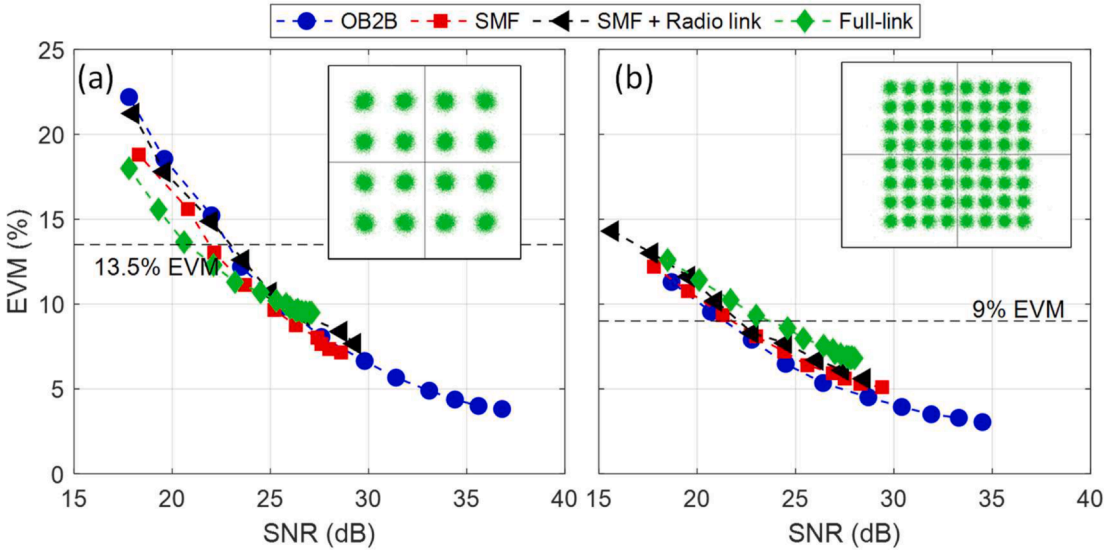

Fig. 7. EVM vs SNR measured for DL with different modulation formats: (a) 16-QAM, (b) 64-QAM. Insets: Constellations of transmitted signals over the full-link with an SNR of 28 dB (16-QAM and 64-QAM).

terms of the RoP and ReP, as well as the SNR, fully validate the network performance and also allow to identify their differences. Results show different power budgets and penalties mainly due to the different structure of DL and UL, where the latter implements electro-optical conversion after amplification of the radio link output signal.

In order to fulfil the 9 % EVM limit for the 64-QAM signals with 20 MHz bandwidth, the minimum received optical power has been determined as −2.7 dBm and −1 dBm in the DL and UL, respectively, for the full-link configuration. It was shown that the advantageous use of the low-frequency DML for the DL and high-frequency DML for the UL to maximize the system performance and simultaneously reduce the complexity. Finally, it has been experimentally demonstrated that the 100 m long FSO channel can be effectively used as the "last mile" access in bidirectional optical fronthaul networks operating at mmW bands to provide better flexibility in the network densification and paves the way to the deployment of future hybrid optical and mobile communication networks operating in the mmW band.

Declaration of Competing Interest

The authors declare that they have no known competing financial interests or personal relationships that could have appeared to influence the work reported in this paper.

Data availability

The authors are unable or have chosen not to specify which data has been used.

Acknowledgment

The research has been supported by the CTU in Prague SGS20/166/OHK3/3T/13, project from Ministry of Industry and Trade in Czech Republic (FV40089) and within COST action CA19111 (NEWFOCUS). It has also been funded by the regional project from Generalitat Valenciana PROMETEO 2021/015 and Grant RTI2018-101658-B-I00 FOCAL by MCIN/AEI/ 10.13039/501100011033 and ERDF "A way of making Europe".

References

[1] W. Jiang, B. Han, M.A. Habibi, H.D. Schotten, The Road Towards 6G: A Comprehensive Survey, IEEE Open J. Commun. Soc. 2 (2021) 334–361.
[2] IMT Traffic estimates for the years 2020 to 2030, ITU-R Standard M.2370-0, 2015.
[3] C. Ranaweera, E. Wong, A. Nirmalathas, C. Jayasundara, C. Lim, 5G C-RAN With Optical Fronthaul: An Analysis From a Deployment Perspective, J. Lightw. Technol. 36 (11) (2018) 2059–2068.
[4] C.H. de Souza Lopes, et al., Non-standalone 5G NR fiber-wireless system using FSO and fiber-optics fronthauls, J. Lightw. Technol. 39 (2) (2021) 406–417.
[5] C. Lim, A. Nirmalathas, Radio-Over-Fiber Technology: Present and Future, J. Lightw. Technol. 39 (4) (2021) 881–889.
[6] M. Giordani, M. Polese, M. Mezzavilla, S. Rangan, M. Zorzi, Toward 6G Networks: Use Cases and Technologies, IEEE Commun. Mag. 58 (3) (2020) 55–61.
[7] T. Nitsche, C. Cordeiro, A.B. Flores, E.W. Knightly, E. Perahia, J.C. Widmer, IEEE 802.11ad: Directional 60 GHz communication for multi-gigabit-per-second Wi-Fi [invited paper], IEEE Commun. Mag. 52 (12) (2014) 132–141.
[8] X. Wang, et al., Millimeter wave communication: a comprehensive survey, IEEE Commun. Surveys Tuts. 20 (3) (2018). Third Quarter.
[9] J. Yao, Microwave Photonics, J. Lightw. Technol. 27 (3) (2009) 314–335.
[10] L. Vallejo, et al., On the 40 GHz Remote versus Local Photonic Generation for DML-based C-RAN Optical Fronthaul, J. Lightw. Technol. 39 (21) (2021) 6712–6723.
[11] H. Kim, J. Song, Full-Duplex WDM-Based RoF System Using All-Optical SSB Frequency Upconversion and Wavelength Re-Use Techniques, IEEE Trans. Microw. Theory Techn. 58 (11) (2010) 3175–3180.
[12] X. Pang, et al., 100 Gbit/s hybrid optical fiber-wireless link in the W-band (75–110 GHz), Opt. Exp. 19 (2011) 24944–24949.
[13] X. Li, J. Yu, J. Zhang, Z. Dong, F. Li, N. Chi, A 400G optical wireless integration delivery system, Opt. Exp. 21 (16) (2013) 18812–18819.
[14] X. Li, J. Yu, J. Xiao, Y. Xu, Fiber-wireless-fiber link for 128-Gb/s PDM-16QAM signal transmission at W-band, IEEE Photon. Technol. Lett. 26 (19) (2014) 1948–1951.
[15] P.T. Dat, A. Kanno, N. Yamamoto, T. Kawanishi, Full-Duplex Transmission of LTE-A Carrier Aggregation Signal Over a Bidirectional Seamless Fiber-Millimeter-Wave System, J. Lightw. Technol. 34 (2) (2016) 691–700.
[16] K.K. Tokgoz, et al., A 56Gb/s W-Band CMOS wireless transceiver, in: Proc. IEEE Int. Solid-State Circuits Conf., 2016, pp. 242–243.
[17] X. Li, Y. Xu, J. Yu, Over 100-Gb/s V-band single-carrier PDM64QAM fiber-wireless-integration system, IEEE Photon. J. 8 (5) (2016) 1–7.
[18] D. del Rio, et al., A Wideband and high-linearity E-B and transmitter integrated in a 55-nm SiGe technology for backhaul point-to-point 10-Gb/s links, IEEE Trans. Microw. Theory Techn. 65 (8) (2017) 2990–3001.
[19] J. Wang, A. Al-Khalidi, L. Wang, R. Morariu, A. Ofiare, E. Wasige, 15-Gb/s 50-cm wireless link using a high-power compact III–V 84- GHz transmitter, IEEE Trans. Microw. Theory Techn. 66 (11) (2018) 4698–4705.
[20] J. Pang, et al., A 28.16-Gb/s area-efficient 60 GHz CMOS bi-directional transceiver for IEEE 802.11ay. Proc. IEEE Asian Solid-State Circuits Conf. (A-SSCC), 2018.
[21] X. Li, J. Yu, L. Zhao, K. Wang, W. Zhou, J. Xiao, 1-Tb/s photonics-aided vector millimeter-wave signal wireless delivery at D-band, in: 2018 Optical Fiber Communications Conference and Exposition (OFC), IEEE, 2018 https://ieeexplore.ieee.org/document/8386377.
[22] C.W. Byeon, K.C. Eun, C.S. Park, A 2.65-pJ/Bit 12.5-Gb/s 60-GHz OOK CMOS transmitter and receiver for proximity communications, IEEE Trans. Microw. Theory Techn. 68 (7) (2020) 2902–2910.
[23] K. Wang, W. Zhou, L. Zhao, F. Zhao, J. Yu, Bi-Directional OFDM Truncated PS-4096QAM Signals Transmission in a Full-Duplex MMW-RoF System at E-Band, J. Lightw. Technol. 39 (11) (2021) pp.
[24] C.T. Tsai, C.C. Li, C.H. Lin, et al., Long-reach 60-GHz MMWoF link with free-running laser diodes beating, Sci. Rep. 8 (2018). Art. no. 13711.
[25] K. Mallick, et al., Bidirectional OFDM Based MMW/THzW Over Fiber System for Next Generation Communication, IEEE Photonics J. 13 (4) (2021) 1–7.
[26] K. Mallick, et al., Bidirectional OFDM-MMWOF transport system based on mixed QAM modulation format using dual mode colorless laser diode and RSOA for next generation 5-G based network, Opt. Fiber Technol. 64 (2021), 102562.
[27] K. Zeb, et al., Broadband Optical Heterodyne Millimeter-Wave-over-Fiber Wireless Links Based on a Quantum Dash Dual-Wavelength DFB Laser, J. Light. Technol. 40 (12) (2022) 3698–3708.
[28] H.-H. Lu, et al., Simultaneous Transmission of 5G MMW and Sub-THz Signals Through a Fiber-FSO-5G NR Converged System, J. Light. Technol 40 (8) (2022) 2348–2356.
[29] J. Kreissl, V. Vercesi, U. Troppenz, T. Gaertner, W. Wenisch, M. Schell, Up to 40-Gb/s Directly modulated laser operating at low driving current: buried-heterostructure passive feedback laser (BH-PFL), IEEE Photon. Technol. Lett. 24 (5) (2012) 362–364.
[30] ETSI Technical specification (TS) 3GPP TS 36.141 version 12.6.0 Release 12: "LTE; Evolved Universal Terrestrial Radio Access (E-UTRA); Base Station (BS) conformance testing, 2015.